

## REVIEW

## Patterning of protein-based materials

Martin Humenik<sup>1</sup>  | Anika Winkler<sup>1</sup> | Thomas Scheibel<sup>1,2,3,4,5</sup> 

<sup>1</sup>Department of Biomaterials, Faculty of Engineering Science, Universität Bayreuth, Bayreuth, Germany

<sup>2</sup>Bayreuth Center for Colloids and Interfaces (BZKG), Universität Bayreuth, Bayreuth, Germany

<sup>3</sup>Bayreuth Center for Molecular Biosciences (BZMB), Universität Bayreuth, Bayreuth, Germany

<sup>4</sup>Bayreuth Center for Material Science (BayMAT), Universität Bayreuth, Bayreuth, Germany

<sup>5</sup>Bavarian Polymer Institute (BPI), Universität Bayreuth, Bayreuth, Germany

**Correspondence**

Thomas Scheibel, Department of Biomaterials, Faculty of Engineering Science, Universität Bayreuth, Prof.-Rüdiger-Bormann-Str. 1, 95447 Bayreuth, Germany.  
Email: thomas.scheibel@bm.uni-bayreuth.de

**Funding information**

Bayrisch-Tschechische Hochschulagentur grant JC-2019-21; Deutsche Forschungsgemeinschaft grant SCHE 603/24-1

**Abstract**

Micro- and nanopatterning of proteins on surfaces allows to develop for example high-throughput biosensors in biomedical diagnostics and in general advances the understanding of cell-material interactions in tissue engineering. Today, many techniques are available to generate protein pattern, ranging from technically simple ones, such as micro-contact printing, to highly tunable optical lithography or even technically sophisticated scanning probe lithography. Here, one focus is on the progress made in the development of protein-based materials as positive or negative photoresists allowing micro- to nanostructured scaffolds for biocompatible photonic, electronic and tissue engineering applications. The second one is on approaches, which allow a controlled spatiotemporal positioning of a single protein on surfaces, enabled by the recent developments in immobilization techniques coherent with the sensitive nature of proteins, defined protein orientation and maintenance of the protein activity at interfaces. The third one is on progress in photolithography-based methods, which allow to control the formation of protein-repellant/adhesive polymer brushes.

**1 | INTRODUCTION**

Patterning techniques have been initially developed for applications in semiconductor industry<sup>[1]</sup> and were later adopted to enable spatiotemporal protein immobilization as well as structuring of protein-based materials. A plethora of techniques are available nowadays to realize protein pattern, such as micro-contact printing,<sup>[2–6]</sup> inkjet printing<sup>[7]</sup> and optical lithography<sup>[8–10]</sup> all of them enabling micro-pattern generation on large-scales. Interferometric lithography,<sup>[11]</sup> electron beam lithography,<sup>[12,13]</sup> dip pen nanolithography,<sup>[14–17]</sup> nanoimprint lithography,<sup>[18,19]</sup> scanning probe lithography,<sup>[20,21]</sup> near-field lithography,<sup>[22,23]</sup> on the other hand provide pattern down to the nanometer scale. The spatiotemporal control of protein

immobilization is crucial for the development of bioanalytic, diagnostic as well as tissue engineering applications.<sup>[24–26]</sup>

Recent developments in surface nano- and microstructuring of protein-based materials will be reviewed as well as the patterning techniques diversely applied on protein-based scaffolds. These techniques rely on specific processivity of a protein material resulting from the introduction of chemical or physical crosslinks or protein structural transformations. Further, recent developments of approaches are provided, which employ a combination of the patterning methods with new chemical tools resulting in 2D and 3D spatiotemporal protein immobilization with concomitant preservation of the protein activity. The basis thereof are specific protein properties such as surface charges, the chemistry of exposed amino acid residues or site-

This is an open access article under the terms of the Creative Commons Attribution-NonCommercial-NoDerivs License, which permits use and distribution in any medium, provided the original work is properly cited, the use is non-commercial and no modifications or adaptations are made.

© 2020 The Authors. *Biopolymers* published by Wiley Periodicals LLC.

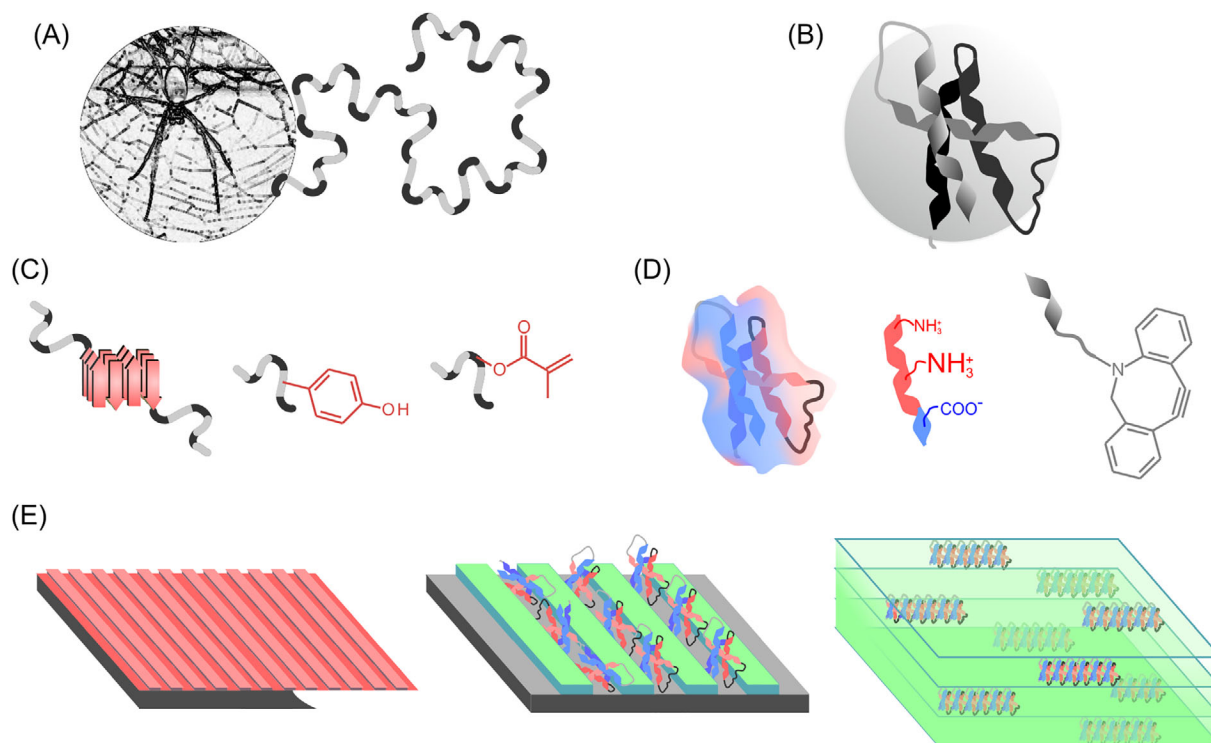


**FIGURE 1** Schematic representation of protein patterning strategies: Structural proteins, such as spider silk in A, or globular proteins, such as enzymes in B, are employed in protein patterning. Structural changes of silk proteins, such as formation of densely packed  $\beta$ -sheets, presence of naturally occurring photosensitive amino acids residues (tyrosines) or introduction of photosensitive modifications (methacrylates) in B, are combined with lithography techniques to prepare patterned protein materials such as microstructured coatings or free-standing scaffolds E (left). Naturally occurring charges on enzyme's surface (red for positive and blue for negative charge) in D (left), chemistry of native amino acids residues such as lysins (red) or aspartic acids (blue) in D (middle) or introduction of bio-orthogonal site-specific modifications, such as cyclooctynes D (right), are employed to immobilize the proteins on correspondingly prepatterned substrates enabling oriented protein pattern on surfaces E (middle) or in hydrogels E (right)

specific incorporation of modifications either genetically or chemically (Figure 1).

## 2 | STRUCTURING OF PROTEIN-BASED MATERIALS FOR APPLICATIONS

Fibrous or so-called scleroproteins represent an important class of proteins next to globular and membrane proteins.<sup>[27]</sup> Collagen, elastin and keratin represent the most abundant proteins in the human body being able to form mechanically stable elastic fibers as supporting structures of tissues and organs.<sup>[27–29]</sup> Other organisms also use fibrous proteins, such as silkworm silk fibroins within cocoons, spider spidroins within webs, or insect resilins within tendons.<sup>[27]</sup> Characteristic for all such proteins are repeating amino acid sequence motifs. Furthermore, self-assembly of these proteins is an intrinsic property allowing a hierarchical self-organization and yielding explicit mechanical properties in the resulting fibrous structures.<sup>[27–29]</sup> The combination of biocompatibility with mechanical robustness has put these protein fibers in the focus of medical and technical applications.<sup>[30–32]</sup> Further, engineering of recombinant variants thereof offers modulation of the amino acid sequence, molecular weights, addition of biological signals, and manipulation of

protein charges, all of which have a severe impact on processability into particles, capsules, foams, nonwoven meshes, films or hydrogels,<sup>[29]</sup> which are applicable in drug delivery, tissue regeneration and optics and electronics, amongst others.<sup>[29–32]</sup>

The patterning of protein-based materials entered the focus of materials' research during the last decade. Simple processing techniques enable the production of highly defined, but also biocompatible micro- and nanostructured substrates for devices. The scalable, high throughput and cost-efficient production makes bottom-up approaches such as soft lithography, photolithography or nanoimprinting the main nanofabrication routes. Despite the simplicity of these lithographic methods, precise structures are achievable with high-resolution pattern at accurate and predefined areas. Common techniques will be summarized in the following paragraphs.

### 2.1 | Patterning of natural proteins

#### 2.1.1 | Patterning using structural transformations

Natural proteins represent a “green” biocompatible and biodegradable alternative for synthetic polymers for various applications. However,

the patterning of protein-based materials such as coatings or free-standing films is still at the beginning of its development in comparison to well established methods using synthetic commercially available polymer resins. Different patterning approaches such as microcontact printing or nanoimprint lithography illuminated the problem of protein stabilization at defined surface areas to achieve high-resolution pattern. Tullii *et al.*<sup>[33]</sup> exploited the simple soft lithographic method to produce microstructured fibroin surfaces. After casting and solidifying of an aqueous silk fibroin solution on a prepatterned poly(dimethylsiloxane) (PDMS) mold, water-insolubility of the protein layer was induced by increasing the crystallinity using water vapor annealing. Honeycomb microstructures were generated ranging from 1 to 5  $\mu\text{m}$  in diameter in microwells. These particular pattern reduced bacterial adhesion up to 66%, whereas mammalian cells adhered and proliferated unaffectedly, as they did on flat surfaces in comparison. The antifouling effect could be traced to the formation of air pockets, which led to a limited contact area between bacteria and the surface.<sup>[33]</sup> Using silk fibroin films, both positive and negative lithography were realized by treatment of the surface with different stamping inks (Figure 2). For positive lithography, first the silk film was stabilized by inducing  $\beta$ -sheet formation with methanol, rendering the film water insoluble. A stamp inked with a denaturation solution

(e.g., strong chaotropic agents such as lithium bromide or sodium thiocyanate solutions) was contact-printed on the silk surfaces in the next step. The localized conformational change from  $\beta$ -sheet to random coil rendered the contact areas water-soluble yielding pattern of the water-insoluble crystalline regions after treatment with aqueous solutions.<sup>[34]</sup> In the process of negative lithography, crosslinking solutions (methanol or ethanol) were stamped directly on nonstructured fibroin films causing the locally increased crystallinity due to the  $\beta$ -sheet formation whereas noncontacted areas could be washed out. In a combination with gold coating, the fabrication of split ring resonators was possible enabling electromechanical and optical systems in a biocompatible, recyclable way.<sup>[34]</sup> Sun *et al.*<sup>[35]</sup> developed a so-called *Patterning on Topography* technique by applying extracellular matrix (ECM) proteins on surfaces of a thermally-sensitive poly(N-isopropylacrylamide) (PIPAAm) flat substrate. Exploiting the PIPAAm's lower critical solution temperature at  $\sim 35^\circ\text{C}$ , the PIPAAm swelling enabled transfer of the ECM protein layer onto and into adjacent microstructures of a PDMS stamp due to hydrophobic interactions. The combination of topological and biochemical pattern on the surfaces was used to study cell-cell and cell-surface interactions in diverse microenvironments.<sup>[35]</sup>

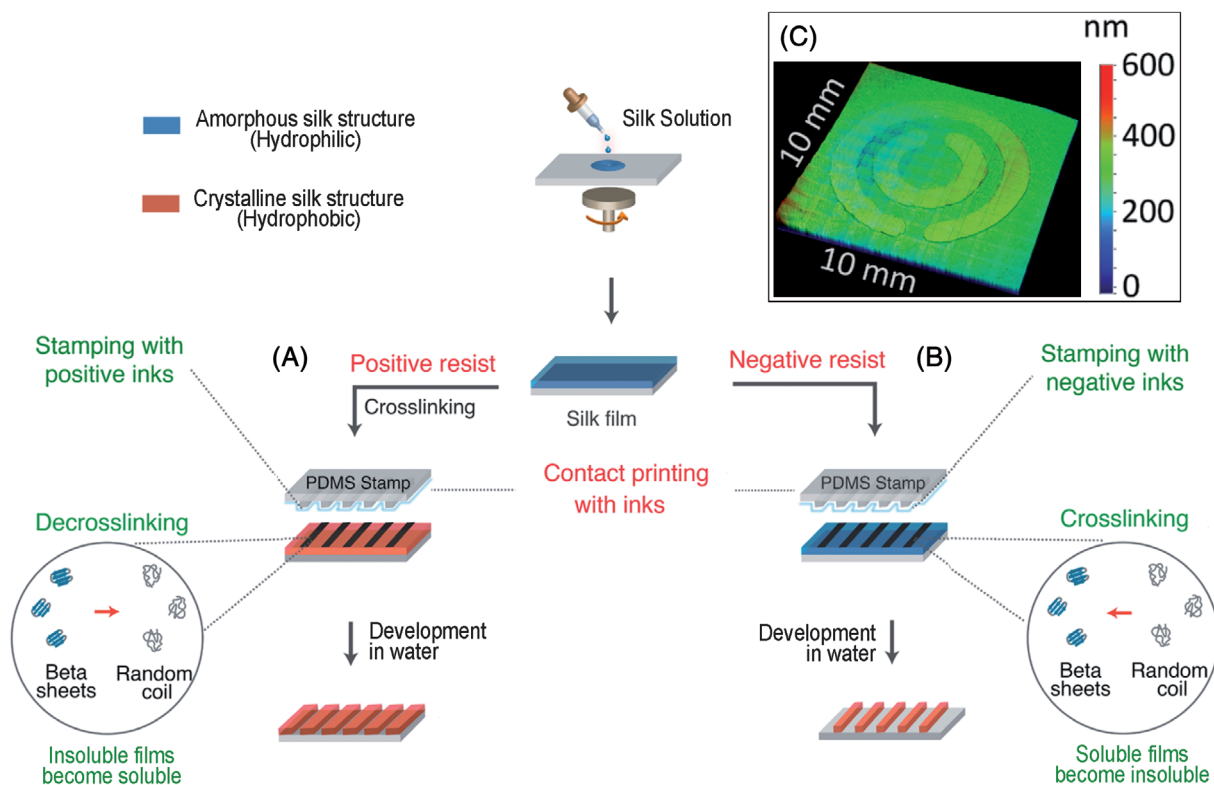


**FIGURE 2** Schematic illustration of the silk microcontact printing process established by Ganesh Kumar *et al.*<sup>[34]</sup> A, To use fibroin as a positive resist, the silk film was physically crosslinked with methanol after coating. The microcontact printing of LiBr as ink led to a conformational change of the silk proteins and increased the water solubility. Water treatment resulted in a positive pattern by removing the printed regions. B, Fibroin as negative resist was microcontact printed with methanol. Crosslinking of the contact areas resulted in an increased crystallinity and a negative protein pattern after development. C, With this approach, split ring resonators for electromagnetic applications could be fabricated (white light measurement with color bar indicating film thickness). Reproduced from Reference [34] with permission of American Chemical Society

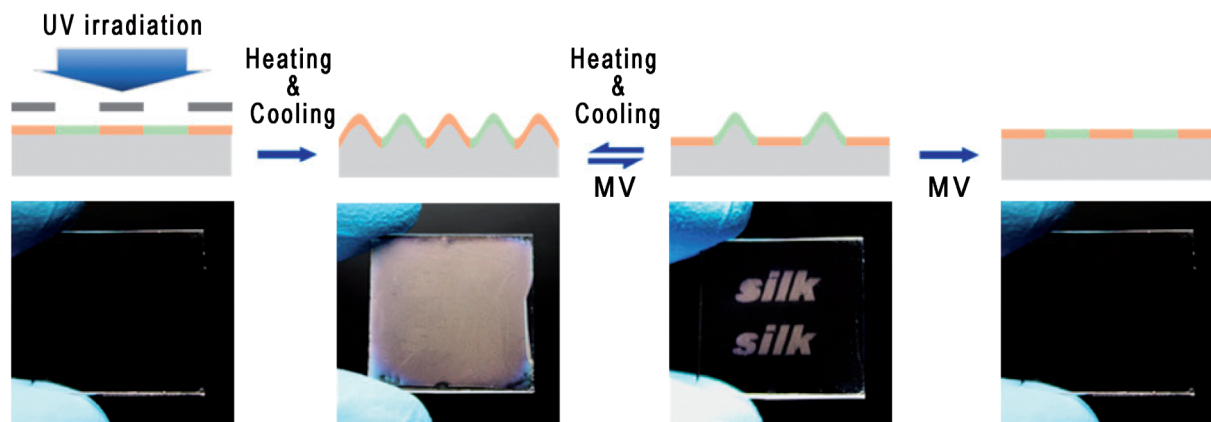


**FIGURE 3** Combined surface wrinkling using silk photolithography for production of smart surface devices. Spin-coating of a thin silk layer on a PDMS substrate resulted in a bilayer system. By heating/stretching and subsequently cooling the layers, wrinkle structures remained on the surface. UV light led to changes in the wrinkle dynamics, whereby wrinkles maintained stable upon short methanol treatment whereas unexposed areas were flattened. Longer methanol exposure permanently erased the wrinkle structures, resulting in a reversible stimuli-responsive system. Reproduced from Reference [37] with permission of National Academy of Sciences

Lithography methods were developed, where exposure of deep-UV light led to breakage of C-N peptide bonds within stable water-insoluble protein films and to a decreased crystallinity. UV-treated areas became soluble and could be washed off by water, which resulted in a well-defined high-resolution protein pattern on a substrate. Due to the positive-tone lithography approach, the incorporation of bioactive or catalytic dopants was possible without impact on the biological function, which enhanced the potential of the patterned silk for biomedical applications.<sup>[36,37]</sup> Wang *et al.*<sup>[37]</sup> developed a fibroin-based wrinkle system, which could be dynamically tuned by methanol vapor or UV irradiation (Figure 3). On a PDMS substrate, a thin fibroin film was applied to form a bilayer system. By heating and subsequently cooling the layers, a labyrinth-like wrinkled surface was achieved. The wrinkling process changed the transparent optical appearance to an opaque one. Wrinkles could be fully eliminated by external stimuli, such as methanol or UV treatment. UV exposure through a photomask enabled defined patterning of the silk surface by removing predetermined areas. The on-demand tunable micro- and nanopattern were completely biocompatible and allowed the fabrication of putatively useful surfaces for medical, mechanical or electrical devices.<sup>[37]</sup>

### 2.1.2 | Patterning using covalent crosslinking of amino acid residues

Crosslinking allows the adjustment of protein materials' properties such as mechanical robustness and resistance against biological degradability for application-specific functions. Traditional radical-based crosslinkers, for instance methylene blue or ruthenium<sup>2+</sup>-based complexes, are often cell toxic and, therefore, less suitable for biomedical applications.<sup>[38]</sup> Glutaraldehyde, known to covalently crosslink lysine residues,<sup>[39]</sup> is also cell toxic. As an alternative, naturally occurring riboflavin, also known as vitamin B2, could act as a visible light-

addressable initiator in photo-crosslinking processes, thus reducing potential damage of the protein integrity during fabrication. The radical-based mechanism is, similarly to other photocatalysts, based on formation of covalent crosslinking of tyrosine residues within the protein backbone into dityrosines.<sup>[40,41]</sup> Applegate *et al.*<sup>[40]</sup> developed a riboflavin initiated photo-crosslinking process of silk fibroin. Improvements in quality and resolution were gained by using high-resolution masks, adjusting the fibroin concentration and exposure times.<sup>[41]</sup> Due to the transparency and elasticity of the fabricated silk layers, applications such as optical prostheses for cornea diseases are conceivable. Curvature and vision could be matched for implants used for certain defects.<sup>[40,41]</sup> Enzyme-mediated crosslinking is another natural and biocompatible alternative. For example, transglutaminases catalyze the reaction of glutamine residues in a protein backbone with primary amines from lysine residues. Micromolded gelatin was crosslinked using microbial transglutaminase and demonstrated an improved myotube guidance for skeletal muscle tissue engineering. The enzymatic crosslinking improved stability and elasticity of the scaffold.<sup>[42]</sup>

## 2.2 | Patterning of recombinant proteins

Utilization of recombinant proteins for creation of patterned material allows implementation of functions which are not available in proteins from natural sources. The genetic manipulation and the recombinant production in predefined host organism enables control over amino acid sequence, molecular weights, as well as fusions with bio-functional domains with, for example, affinity or light emitting functions. Thus, the employment of recombinant variants provides further tuning space of lithography processes in order to achieve higher precision of the patterned structures and bio-functional surfaces.

A precise nanostructuring was achieved with surfaces made of genetically engineered spider silk variants having 16 repetitive

consensus sequence modules flanked by the N- and C-terminal domains of the spider *Nephila clavipes* dragline silk protein MaSp1. Accurately directed ion and electron beam interactions with the protein's matrix at the nanoscale enabled to create well-defined 2D and 3D nanopattern. The control over protein sequence and molecular weight of the recombinant spider silk variants via genetic engineering provided lithographic resolutions approaching the molecular limit. The aqueous recombinant spider silk solutions could be further functionalized with a variety of chemical and biological dopants such as fluorescent dyes, enzymes, and antibodies through simple mixing before their processing into nanostructured coatings. This approach provided a facile method for patterning and immobilization of functional molecules within nanoscopic, hierarchical silk structures, enabling biomedical applications such as structure-enhanced fluorescence and biomimetic microenvironments for controlling cell fates.<sup>[43]</sup>

Technically less demanding methods use soft lithography with PDMS molds to process micropattern of recombinant protein materials. For instance, a functional amyloid protein CsgA was used to develop a material platform for producing hierarchically ordered fibrous microstructures.<sup>[44]</sup> CsgA is a protein expressed in *Escherichia coli*, which naturally self-assembles into functional amyloid fibers forming an extracellular matrix encapsulating the bacteria within a biofilm.<sup>[45]</sup> Using a combination of soft lithography with CsgA monomer inks, the protein could be transferred onto surfaces. A methanol-assisted curing of the imprinted CsgA pattern enabled the in situ reassembly of amyloid monomers on the surfaces. The resulting patterned structures exhibited chemical, thermal and mechanical stability at harsh conditions. The robustness of the CsgA self-assembly enabled also the fusion with tags such as a polyhistidine-tag fused to the C-terminus of CsgA for binding of inorganic nanoparticles, or CsgA-CBD with a fused chitin-binding domain (CBD) acting as a linker between chitin and CsgA nanofibers and enabling self-supporting patterned porous sheets.<sup>[44]</sup>

Another example represents native and recombinant squid ring teeth (SRT) proteins exhibiting reversible solid-to-melt phase transition and thermal processability into different micro- to macroscopically shaped materials.<sup>[46,47]</sup> Using PDMS molds, the thermoplastic (SRT) proteins could be cast on the negative mold and formed a free-standing film with microstructures of whispering-gallery-mode (WGM) resonators. Their thermorefractivity increased with  $\beta$ -sheet crystallinity altered by methanol exposure and it was generally higher for the recombinant SRT proteins than for their native counterpart. The WGM resonators made of the SRT proteins were applied in waveguides in add-drop filters that are frequently integrated in optical filters.<sup>[48]</sup> Submicron-sized pattern could be also imprinted into soft, recombinant elastin-like protein-based (ELP) hydrogels. Transferring aligned and unaligned wavy pattern from PDMS molds to the bio-responsive soft ELP-based material enabled topographical cell response studies with adipose-derived stem cells at elastic moduli matching those of tissues. The periodicity limit of the pattern was set by inherent protein assemblies (diameter: 124–180 nm) formed due to lower critical solution temperature behavior of the ELP during the molding process.<sup>[49]</sup>

PDMS stamps could also be used for micromolding in capillaries (MIMIC) allowing to form complex microstructures in the stamp capillaries upon contact with surfaces.<sup>[50,51]</sup> MIMIC was established in combination with coatings based on recombinant spider silk and lacing egg stalk proteins processed into patterned silk scaffolds to shape and organize cells, such as mouse fibroblasts and myoblasts.<sup>[51]</sup> Recently, our group used different engineered eADF3 and eADF4 variants (derived from *Araneus diadematus* fibroin 3 and 4, two main protein components of the dragline fiber of the European garden spider) in combination with MIMIC to produce structured films with tunable  $\beta$ -sheet crystallinity. The analyses of the surfaces clearly showed that both smooth and patterned films made of positively or negatively charged eADF4 variants substantially restricted the attachment, growth and microbial colonization of pathogenic bacteria as well as fungi, and confirmed the superior repellence of spider silk surfaces if compared to those of *Bombyx mori* fibroin and PCL materials. Further, designed spider silk materials with fused cell adhesion motives (e.g., RGD) promoted specific mammalian cell attachment and proliferation while inhibiting microbial infestation.<sup>[52,53]</sup>

### 2.3 | Patterning of photoresists based on chemically modified proteins

Crosslinking agents in combination with naturally occurring amino acid residues usually introduce unspecific inter- and intramolecular bonds in a random arrangement in proteins. However, for fabrication of application-specific nano- and micropatterned surfaces reproducibility of the process is decisive. Thus, a defined chemical manipulation of the proteins helps to generate constructs with accurate high-resolution structures.

Fibroin protein photoresist (FPP) was obtained by chemical modification of native silk fibroin via predefined introduction of a photo-reactive methacrylate group. Patterned surfaces could be fabricated using photomasks and FPP as a negative photoresist upon exposure to UV light. Crosslinked and stabilized structures were achieved in defined pattern at the micro- to macroscale ( $\mu\text{m-cm}$ ).<sup>[54]</sup> The same strategy was applicable for the silk glue protein sericin in form of a sericin protein photoresist (SPP).<sup>[55]</sup> Due to their transparency, mechanical robustness and biocompatibility, the combined use of FPP and SPP facilitated the production of cost-efficient and biofriendly optical systems. In natural systems, optical behavior is traced to periodically structured materials by manipulation of light, for example, based on diffraction or interference.<sup>[56]</sup> Using photolithography, this system could easily be transferred to flexible soft substrates, and they could be utilized as optical microlenses or photonic microdevices. Pal *et al.*<sup>[57]</sup> demonstrated micropatterning of silk protein photoresists (FPP and SPP) for the production of Fresnel zone plates (FZP) for light focusing. FZPs are used for laser and X-ray concentration in imaging applications (Figure 4). Thereby, light was diffracted when passing radially transparent zones, whereas arrangement of the zones was designed to create constructive interference amplifying the radiation.<sup>[57]</sup> Upon further optimization of processing parameters during

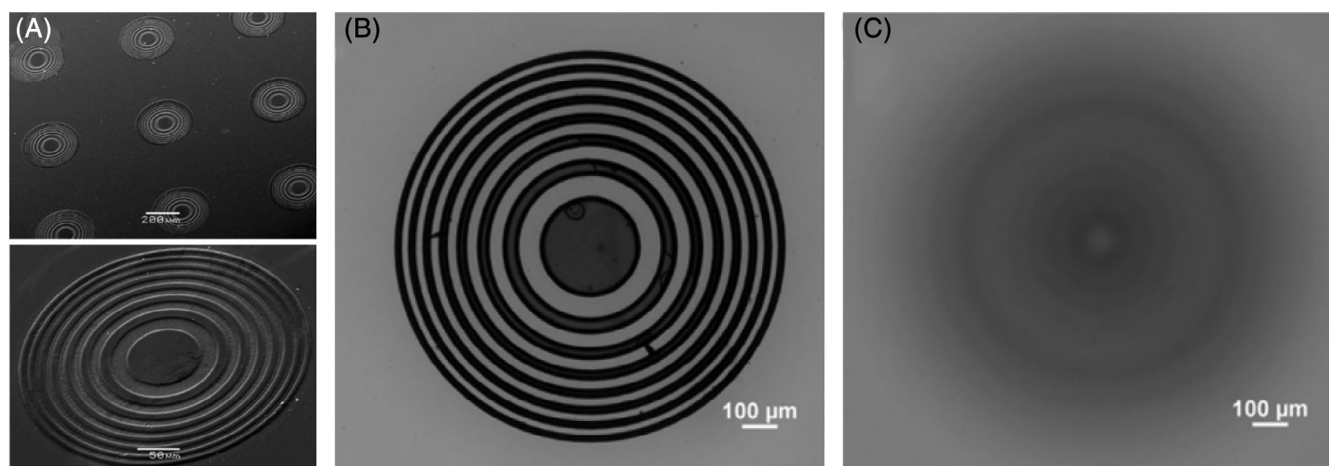


**FIGURE 4** Fresnel Zone Plate fabricated using silk protein photolithography. SEM and optical images of the Fresnel lenses A and B, upon light focusing by the lens C. Reproduced from Reference [57] with permission of American Chemical Society

the micropatterning processes such as solvents<sup>[58]</sup> as well as quality and molecular weight of the precursor protein,<sup>[59]</sup> materials tuning could be driven by the application. Additionally, the introduction of metals, biodopants, drugs, functional molecules, or polymers without activity-loss was possible due to potential implementation of negative-tone lithography.<sup>[59,60]</sup> Choosing proper pattern made of silk-based resists to optimize cell guidance helped to understand dynamic cell processes and interactions.<sup>[55,59,61]</sup> Aside of silk and sericin, the methacrylation was also used to modify wool keratin (WK). Next to properties such as good biocompatibility, high mechanical robustness and biodegradability, the use of WK photoresist as biomaterial has the advantage to include several cell binding motives, making micropattern of WK materials highly suitable for cell culture studies.<sup>[62]</sup> Chemically modified gelatin carrying a photo-reactive azido phenyl group (P-gel) was processable upon UV crosslinking. Neuronal growth factors (NGF) incorporated into a patterned P-gel material enabled guided neurite formation dependent on the micropatterned structure with advantages for the treatment of degenerative diseases and neuron damages after accidents.<sup>[63]</sup>

### 3 | DEFINED SPATIOTEMPORAL IMMOBILIZATION OF ACTIVE PROTEINS ON INTERFACES

#### 3.1 | Protein patterning using nonspecific immobilization

##### 3.1.1 | Patterning using protein adhesion

Irradiation with a mask or digital light projection for triggering of photochemical reactions are frequently used for surface activation resulting in predefined protein pattern. The photolithographic methods provide the spatial and the temporal control, are noninvasive, scalable and cost-efficient. Two principal approaches were

developed, either removal or polymerization of the protein nonfouling materials. Resulting protein adhesive/repellent surfaces allowed physical or chemical binding of proteins in a nonoriented manner.

Light-induced molecular adsorption (LIMAP) has been developed using several chemical principles. Application of water-soluble photoinitiators and UV-light enabled tuning of antifouling properties of poly(L-lysine)-graft-poly(ethylene glycol) brushes (PLL-g-PEG) applying a photoscission mechanism.<sup>[64]</sup> The degradation of the PEG moiety was UV-dose dependent resulting in controllable protein adsorption.<sup>[65]</sup> High resolution wide-field digital micromirror device (DMD) projection enabled generation of arbitrary grayscale pattern, which were used to perform selective immuno-assays, to dynamically control the adhesion of individual cells, and to achieve hierarchical cocultures (Figure 5A,B).<sup>[65]</sup> Photodeprotection of the PLL-g-PEG-based brushes was achieved also by introducing a photosensitive nitrophenylethoxycarbonyl linker on aminopropyltriethoxysilane. The proteins were deposited on the deprotected aminated spots with high selectivity. Multiple geometric pattern with up to four different fluorescently labeled proteins were possible using sequential application of near-field photolithography.<sup>[67]</sup> Photocatalytic self-cleaning properties of Titania could also be exploited on SiO<sub>2</sub>-substrates with titanium dioxide nanopattern passivated first with oligo(ethylene glycol). Deprotection of the TiO<sub>2</sub> nanostructures upon near-UV irradiation enabled UV-controlled absorption and removal of fluorescently labeled proteins. The approach is for instance suitable for preparation of reusable nanostructured biological interfaces.<sup>[68]</sup>

Although frequently used, the high energy UV-light is not well compatible with biomaterials due to possible impact on their chemical and physical properties. Thus, longer wavelengths in VIS and near-infrared spectral regions, bearing correspondingly less energy, are preferable to preserve protein functionality upon processing of pattern. Due to broadly tunable spectral sensitivity, ruthenium complexes allowed already the development of several photo-responsive materials.<sup>[69]</sup> Such complexes immobilized on surfaces could be also used to configure protein adhesive and repellent patches. Near IR-light-

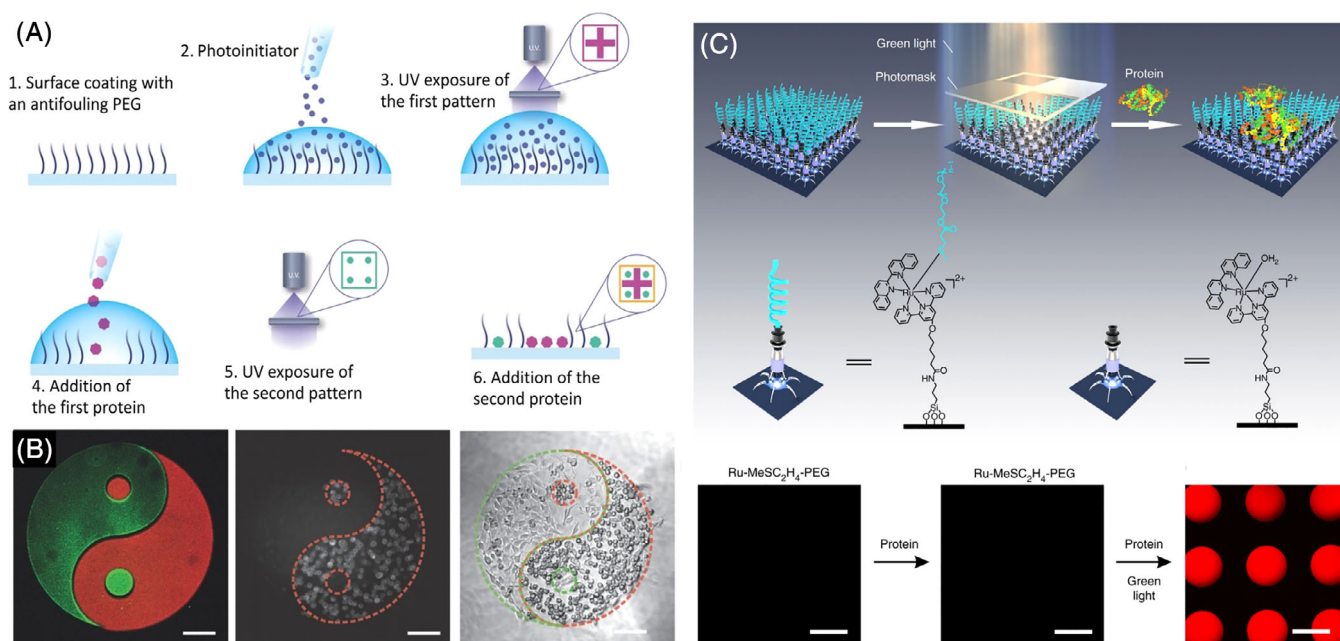


**FIGURE 5** Protein patterning via nonspecific protein adhesion. A, Schematic representation of light-induced molecular adsorption (LIMAP) patterning using (1) PLL-g-PEG brushes deposited on a glass cover-slip; (2) Addition of Lithium phenyl-2,4,6-trimethylbenzoylphosphinate (LAP) photoinitiator; (3) UV light irradiation creating first adhesive spots for the first protein pattern (4); Repetition of the process enables protein multipattern (5-6); B, LIMAP orthogonal patterning of adhesion proteins. Left panel: Epifluorescence microscopy of a two-protein pattern composed of Cy3-labeled fibronectin (FN) (red) and Alexa-488-labeled streptavidin (green); Middle panel: Epifluorescence microscopy image showing GFP expressing cells stably adhering only to the FN pattern. Right panel: Phase contrast images showing the second cell line adhering after incubation with biotinylated FN. Scale bar: 100  $\mu\text{m}$ . C, Schematic illustration of the conversion of a protein-resistant surface containing  $\text{Ru}^{2+}$  complexes with a thioether-terminated protein repellent polyethylene glycol ligand ( $\text{MeSC}_2\text{H}_4\text{-PEG}$ ) into a protein-adsorptive surface after a coordination exchange with water molecules after irradiation with visible light. The process was visualized using fluorescent microscopy: Left panel, the fluorescent images of the  $\text{Ru}^{2+}\text{-MeSC}_2\text{H}_4\text{-PEG}$ -modified surface; Middle pane,  $\text{Ru-MeSC}_2\text{H}_4\text{-PEG}$ -modified surface after immersion in a solution of fluorescently labeled BSA; Right panel: The protein pattern after irradiation through a photomask. Scale bars are 300  $\mu\text{m}$ . A and B, reproduced from Reference [65] with permission of WILEY-VCH Verlag GmbH & Co.; C, reproduced from Reference [66] under the permissions of Creative Commons Attribution 4.0 International License: <http://creativecommons.org/licenses/by/4.0/>

induced photochemistry assisted by lanthanide-doped upconverting nanoparticles enabled cleavage of positively charged  $\text{Ru}^{2+}$  complexes with bound negatively charged proteins using a photomask.<sup>[70]</sup> Visible-light-controlled  $\text{Ru}^{2+}$ -thioether coordination chemistry was also used to endow a  $\text{Ru}^{2+}$ -modified substrate with different functional ligands. To change the surface function, an immobilized PEG ligand was cleaved from the substrate using visible light resulting in spatially controlled protein adsorption (Figure 5C,D).<sup>[66]</sup> Besides the irradiation, focused thermal energy could be used for spatially defined deprotection of surfaces. Applying thermochemical scanning probe lithography, amine pattern were generated on a methacrylate copolymer film. Sulfonate functionalized proteins were then directly immobilized on the amine pattern with sub-10 nm line width using electrostatic interactions.<sup>[71]</sup>

Contrary to the deprotection strategies, the spatiotemporal polymerization or capture of nonfouling polymers have also been employed to create defined polymer/protein interfaces. Specific phase transition of lysozyme<sup>[72]</sup> has been induced for the prepriming of a variety of substrates deficient in C—H bonds such as quartz, gold, glass, silicon and ITO (indium tin oxide). Resulting high C—H density enabled Norrish-type photografting of protein repellent poly[oligo

(ethylene glycol) methyl ether methacrylate] (POEGMA). The patterned surfaces were exposed to FITC-conjugated proteins yielding selective adsorption to the interspaces of POEGMA brush layers. The efficiency of the process, however, depended on the solution pH, which had to be adjusted to make proteins negatively charged.<sup>[73]</sup> Thiol-yne photoclick reactions<sup>[74]</sup> were employed successfully for surface modifications with hydrophilic and hydrophobic regions<sup>[75]</sup> as well as protein coupling on polymer brushes.<sup>[76-78]</sup> For example, well-defined superhydrophilic pattern based on 1-thioglycerol on a superhydrophobic background of 1H,1H,2H,2H-perfluorodecanethiol were generated on rough alkyne-modified ITO substrates. Grafting from the hydrophilic spots via surface-initiated atom-transfer radical polymerization (SI-ATRP)<sup>[79]</sup> yielded PIPAAm pattern with a thermo-responsive hydrophilic to hydrophobic transition. The engineered surfaces were tested as smart MALDI-TOF plates for on-plate desalting and enrichment of digests of different proteins and peptides.<sup>[80]</sup>

Micropatterned PDMS stamps represent a simple approach to transfer a protein of interest onto surfaces.<sup>[81-84]</sup> Recently, the simple soft lithography technique was used for creation of protein repellent/adhesive interfaces employing a marine mussels' adhesive mechanism. The marine mussels' tight binding to various substrates in aqueous

environment relies on repeated 3,4-dihydroxy-L-phenylalanine (DOPA) residues in mussel adhesive proteins, and DOPA patches provide a versatile tool for surface modifications.<sup>[85]</sup> Polydopamine (PDA) on PDMS stamps were easily imprinted to several substrates such as glass, silicon, gold, polystyrene, and poly(ethylene glycol). PDA pattern imprinted on cytophobic (polystyrene) and nonfouling substrates (PEGylated surfaces) were used to form pattern of cells or proteins.<sup>[86]</sup> Micropattern of hydrophilic polymer brushes made of [poly(acrylic acid), poly(hydroxyethyl acrylate) and poly(tetraethylene glycol acrylate)] were achieved using MIMIC. The hydrophilic polymers were covalently bound on cyclopentadienide-modified surfaces using a rapid hetero Diels-Alder (HDA) reaction. Since hydrophilic polymers typically prevent protein adsorption,<sup>[87]</sup> the achieved pattern revealed passivation against biological impact in well-defined areas as demonstrated by adsorption of rhodamine-labeled peanut agglutinin. Moreover, the polymer brushes could be detached at elevated temperatures because of the reversibility of the HDA reaction.<sup>[88]</sup>

### 3.1.2 | Covalent protein binding

Photoinitiated growth of polymer brushes on surfaces has been employed to establish suitable biorthogonal groups on surfaces enabling a covalent protein immobilization. Photocatalytic SI-ATRP<sup>[79]</sup> enabled hierarchical polymer brushes composed of a bottom antifouling block and a top polymer carrying a biorthogonal functional group. For example, architectures build on the inert bottom block of monomethoxy oligo(ethylene glycol) methyl ether methacrylate and the top block of 3-azido-2-hydroxypropyl methacrylate were employed in protein patterning using a strain-promoted alkyne-azide cycloaddition (SPAAC) reaction. The polymerization of the azide containing polymer brush could be defined by DMD resulting in spatial modulation of the azide group density and consequently of the surface-bound biomolecules prefunctionalized with dibenzocyclooctyne (DBCO).<sup>[89]</sup> The protein patterning on such surfaces could also be defined by contact printing using for instance polymer pen lithography.<sup>[90]</sup>

Utilization of electron beam lithography (EBL) required the development of resist materials being water soluble and protecting biomolecules from denaturation during irradiation and high vacuum. Thus, a polystyrene backbone, known to act as a negative-tone resist, was conjugated with pendant trehalose units and shown to effectively stabilize different classes of proteins such as enzymes, growth factors and immunoglobulins during the harsh EBL processing steps.<sup>[91,92]</sup>

## 3.2 | Patterning based on site-specific protein immobilization

Unspecific immobilization enables only indiscriminate binding of all proteins from the environment. Moreover, ill-defined interactions between proteins and substrates, unpredictable unfolding of proteins, and wrong orientation on the substrate cause loss of activity. Thus,

enzyme immobilization on surface pattern with predefined configurations showed significant improvement in fabrication of functional biosensors and protein microarrays.<sup>[93–96]</sup> Protein modification strategies<sup>[97–99]</sup> incorporating site-specific tags in proteins could be combined with patterning strategies exposing corresponding coupling counterparts on surfaces. Furthermore, due to the sensitive nature of proteins, patterning protocols are preferred, which keep the proteins in an aqueous environment during their immobilization.

A short affinity tag consisting of polyhistidine residues (His-Tag) on recombinant proteins allows their metal-affinity chromatography (IMAC)-based purification.<sup>[100]</sup> Specific interactions between Ni<sup>2+</sup> complexes of nitrilo-triacetic-acid (Ni-NTA) groups on surfaces and the His-tag, which is introduced site-specifically into the protein-of-interests on the genetical level, has been used in diverse immobilization schemes<sup>[101,102]</sup> and in protein patterning as well.<sup>[103]</sup> However, beside the site-specificity of the protein immobilization, the use of noninvasive wavelengths should be addressed to preserve functionality of the proteins. Promising approaches are represented by the utilization of photosensitive proteins, which change their quaternary structures upon absorption of visible light. Such proteins, for example, Light-oxygen-voltage domain LOV2<sup>[104]</sup> (blue light), Dronpa<sup>[105]</sup> (violet and cyan light) or Phytochrome-like protein Cph1<sup>[106]</sup> (red light) allowed reversible control of hydrogel material properties.

His-tagged green light cleavable protein tetramer CarH, derived from a photosensitive transcriptional repressor, has been used for protein patterning (Figure 6). The specificity of His-tag/Ni-NTA interaction allowed oriented immobilization of active proteins. Since CarH dissociates at green light into monomers, the release of the proteins-of-interest in the upper layers has been achieved employing a photomask. The reversibility of Ni-NTA binding enabled complex pattern of different fluorescent proteins. Protein pattern made of fibronectin allowed spatial control of cell adhesion.<sup>[107]</sup> The importance of the His-tag placement on the protein structure in relation to the protein coverage density as well as protein activity on a patterned surface has been systematically studied using His-tagged red fluorescent proteins (TagRFP). It has been shown that the binding strength increased by one order of magnitude for each additional His-tag on the protein-of-interest.<sup>[108]</sup> Although highly specific, the bioaffinity approaches represented by the His-tag/Ni-NTA or biotin/streptavidin pairs<sup>[93]</sup> are based on noncovalent interactions. Whereas the efficacy of the Ni-NTA method is limited due to the low binding affinity and heavy metal-dependency, the bulky streptavidin and its tetravalent biotin binding could result in heterogeneous surface coverage and unspecific absorption of a protein-of-interest. In the recent two decades, several biotechnologically accessible protein tags have been established enabling site-specific and covalent protein modifications.<sup>[98,99]</sup> Such strategies could be also exploited in protein patterning (see also Section 2.3). For example, SpyTag/-Catcher and SnoopTag/-Catcher pairs are self-ligating high-affinity peptides which form a covalent bond between unique lysine and aspartic acid residues of each fragment.<sup>[109,110]</sup> Recently, SpyTag and SnoopTag modifications of a bacterial hydrophobin BslA have been exploited in parallel to create patterned surfaces. Those

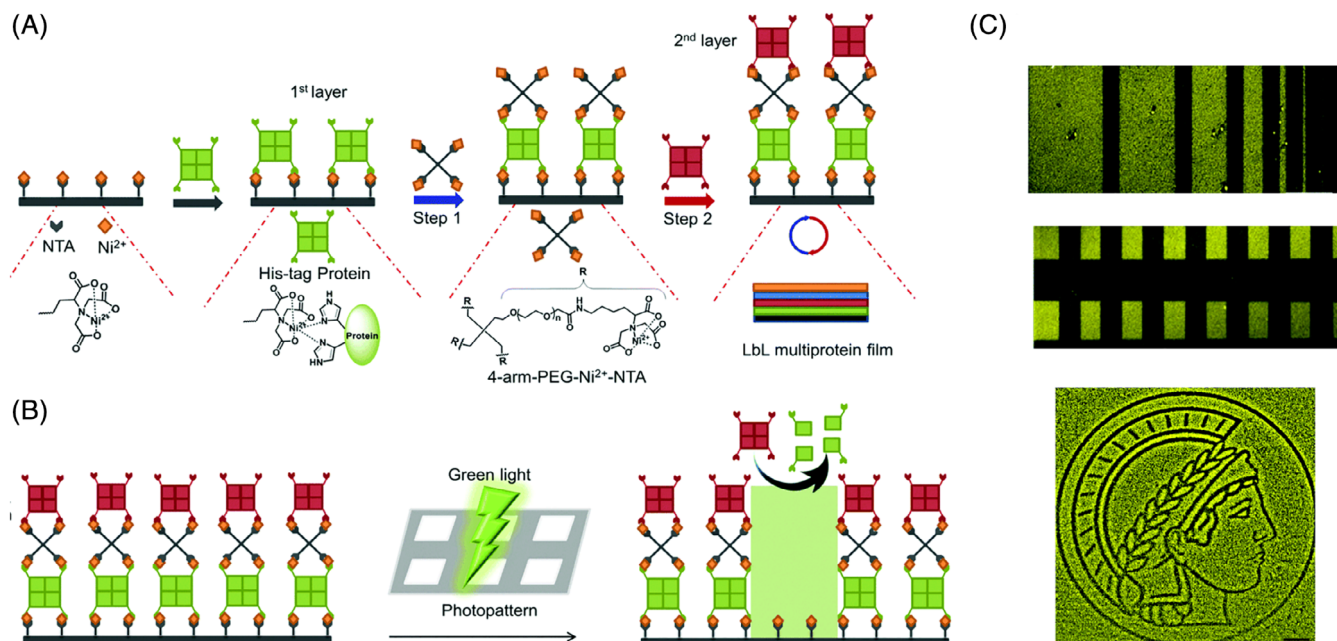


**FIGURE 6** Strategy for green light lithography and the assembly of LbL multiprotein films. A, The LbL multiprotein films were assembled using the multivalent interactions between 4-arm-PEG- $\text{Ni}^{2+}$ -NTA and multimeric His-tagged proteins. A protein with multiple His-tags is immobilized on a  $\text{Ni}^{2+}$ -NTA functionalized surface to form the first protein layer. Subsequent layers are formed by alternately adding 4-arm-PEG- $\text{Ni}^{2+}$ -NTA (Step 1) and a protein of interest with multiple His-tags (Step 2). B, The green light cleavable protein CarH, which is a tetramer in the dark, is incorporated into the first layer. Proteins in the upper layers can be removed locally by projecting a pattern of green light on the LbL multiprotein film. C, Proteins were locally patterned by projecting different pattern using digital micromirror device: Upper panel, pattern with thickness of 100 to 1  $\mu\text{m}$  separated by 20  $\mu\text{m}$  gaps; Middle panel, Stepwise patterning of 40  $\mu\text{m}$  vertical lines and 80  $\mu\text{m}$  horizontal lines yielding a cross protein pattern; Bottom panel, logo of the Max Planck Society. The removal of the fluorescent protein TurboRFP from the illuminated areas leads to a dark protein pattern on a bright background. Scale bar: 100  $\mu\text{m}$ . Reproduced from Reference [107] under the permission of Creative Commons Attribution 3.0 Unported License <https://creativecommons.org/licenses/by/3.0/>

surfaces were functionalized specifically with fluorescent proteins SpyCatcher-eGFP and SnoopCatcher-mCherry, respectively, enabling presentation of the recognition elements in uniform, active conformations.<sup>[111]</sup>

Another approach is the site-specific coupling of DNA oligomers to proteins, which allows for the precise control of protein orientation.<sup>[112]</sup> DNA-directed protein immobilization so far has enabled numerous applications in biosensing and biomedical diagnostics as well as fundamental studies in biology and medicine on the single-cell level.<sup>[113,114]</sup> Recent developments employed specific chemical modifications of DNA for creating protein patterned surfaces.

Oligonucleotides terminally functionalized with photo-caged dienes were shown to react quantitatively with maleimides in a light-induced Diels-Alder cycloaddition in aqueous solution and enabled DNA photopatterning using direct laser writing. Functional DNA arrays were further encoded with fluorophores and proteins through DNA directed immobilization.<sup>[115]</sup> Intrinsic photosensitivity of aromatic bases could be also exploited to produce interstrand cross-linking for creating photo-patterned surfaces.<sup>[116,117]</sup> Recently, a DNA double-write process has been established, which utilized UV irradiation to pattern a specifically designed DNA writing material. The mechanism is based on UV-induced thymine dimerization resulting in

prevention of corresponding base-pairing. Applying complementary fluorescent protein-DNA conjugates, pattern were created using a photomask.<sup>[118]</sup> Our group realized bottom-up protein-based self-assembly in predefined pattern. Recombinant spider silk protein (rssp) eADF4(C16) was conjugated with short DNA strands using azide-alkyne click chemistry (Figure 7A).<sup>[119,120]</sup> DNA-rssp conjugates were hybridized on silica surfaces functionalized with complementary DNA using micro-contact printing with wrinkled PDMS stamps. Deposited conjugates and intrinsic properties of eADF4(C16) enabled nucleated self-assembly of the rssp on predefined surface spots resulting in pattern of beta-sheet-rich fibrils with high contrast and submicron precision (Figure 7B,C).<sup>[121]</sup>

### 3.3 | 3D patterning in hydrogels

Hydrogels utilized in drug delivery, tissue engineering, and molecular diagnostics<sup>[122–124]</sup> represent suitable scaffolds for embodiment of active biomacromolecules such as antibodies, enzymes or nucleic acids aptamers.<sup>[125–127]</sup> High surface area, porosity and water content enable a native-like environment with low spatial restrictions of immobilized biomacromolecules and high substrate diffusion rates,<sup>[120,123,124]</sup> which is in contrast to many conventional surface-

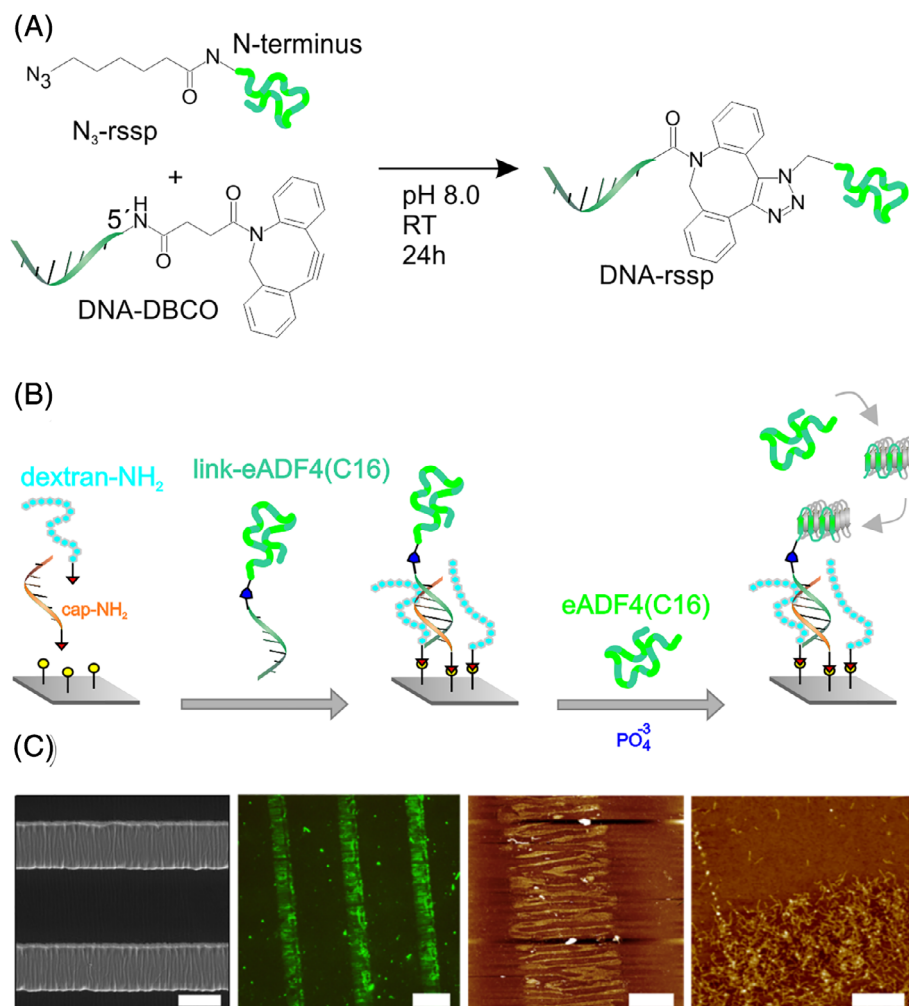


**FIGURE 7** A, Coupling of azide-modified recombinant spider silk proteins ( $N_3$ -rssp) with 5'-dibenzocyclooctyne-modified DNA (DNA-DBCO) yields hybrid building blocks; B, Schematic representation of a patterning strategy for localized fibril self-assembly. An epoxy-activated Si-surface was modified using capture 5'-amino oligonucleotides (cap-ODN) and passivated using low molecular weight amino dextran. A PDMS stamp inked in complementary oligonucleotide-spider silk conjugate link-eADF4(C16) was used to bind the spider silk moiety to predefined spots. Addition of phosphate ions and the monomeric spider silk protein eADF4(C16) triggered silk assembly into  $\beta$ -sheet-rich fibrils on the spotted conjugates. C, From left to right: Detail of the wrinkled PDMS stamps; Fluorescence microscopy of DNA-eADF4(C16) patterned features enhanced after incubation with fluorescein-labeled eADF4(C16) suggesting the presence of substructures within the pattern; AFM characterization of features at different length scales. Scale bars, 20, 50, 10, and 0.6  $\mu\text{m}$ . A, Reproduced from Reference [118] under the permission of the Creative Commons CC-BY-NC-ND license; B and C, Reproduced from Reference [119] under the permission of American Chemical Society

based approaches used in biosensor development facing limitations related to nonspecific adsorption and/or denaturation of biomacromolecules resulting in restricted bioactivity.<sup>[128,129]</sup> Hydrogels, as highly hydrated and cross-linked polymeric networks, represent promising candidates to mimic the ECM, which can be used in tissue engineering.<sup>[130]</sup> Therein, light is an ideal stimulus to define the immobilization of biofunctional groups because it can be controlled in time and volume space using, for example, advanced multiphoton lithography techniques.<sup>[131–134]</sup>

In one example, proteins were adsorbed in pattern employing Coumarin-caged lysine betaine zwitterions. The photosensitive cationic monomer, incorporated into a polyvinylpyrrolidone hydrogel, could controllably change the charge from an adhesive cationic state to a non-adhesive zwitterionic state upon irradiation at 365 nm. With this strategy, the immobilization of proteins with a  $pI < 7$  could be demonstrated. Further, adhesion could be programmed on hydrogels using fibronectin as a biofunctional group. Utilization of photomasks and UV-light enabled, however, only a low patterning depth in the range of few micrometers.<sup>[135]</sup> Covalent protein patterning was demonstrated in PEG hydrogels prepared using SPAAC with incorporated allyl sulfide moieties (Figure 8A) suitable for photomediated thiol-ene photoconjugations.<sup>[74]</sup> The proteins were nonspecifically thiolated on exposed lysine residues

and patterned in the hydrogel. Subsequent photocontrolled thiol-ene reaction with a PEG thiol enabled repeated protein binding through multiple iterations at physiologically relevant conditions (Figure 8B,C).<sup>[136]</sup> Using the SPAAC, UV photosensitive *o*-nitrobenzyl derivatives were also implemented in protein-resistant PEG hydrogels enabling spatiotemporal generation of aldehyde-rich regions and immobilization of unmodified proteins using nonspecific imine ligation and were independent of the  $pI$  value the proteins.<sup>[125,138]</sup> Human umbilical vein endothelial cells (HUVEC) and human fibroblast (HFF-1) were selected as cellular models and adhered to patterned gelatin, FN, and collagen, respectively.<sup>[138]</sup>

Development of hydrogel patterning using VIS wavelengths enabled the increase of patterning depth and cytocompatibility. Exemplarily, a photocleavable protein (PhoCl) was used, which undergoes backbone photocleavage at  $\lambda \approx 400$  nm. Different photoreleasable proteins were fused with the PhoCl C-terminus, whereas the N-Terminus was modified with an azido group using N-myristoyltransferase (NMT) enabling site-specific tethering into SPAAC-based PEG hydrogels. Using a photomask or laser-scanning lithography, proteins were released in complex pattern and gradients through the entire thickness (0.5 mm) of the gels (Figure 8D-F). A photopatterned epidermal growth factor presentation was exploited to promote anisotropic cellular proliferation in 3D.<sup>[137]</sup> Stepwise

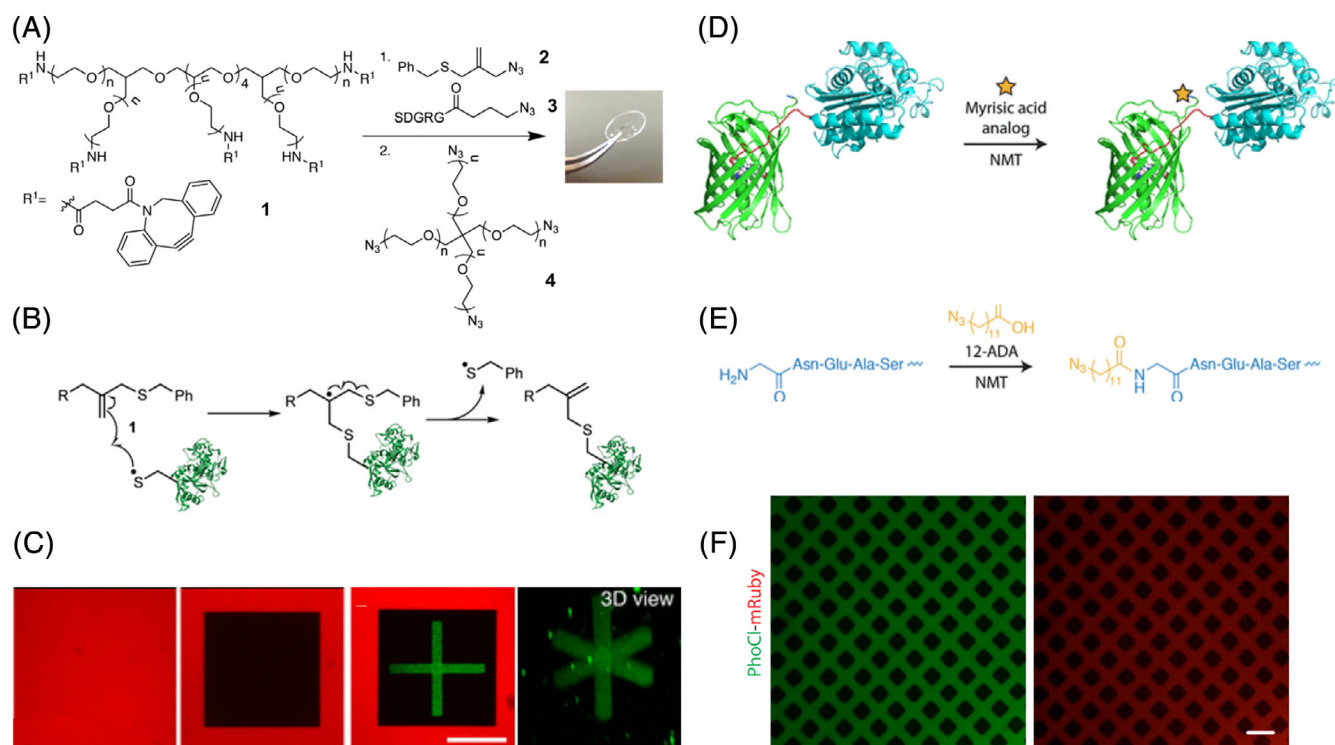


**FIGURE 8** A, Synthesis of allyl sulfide hydrogels employing SPAAC polymerization. Eight-armed PEG<sub>40K</sub>-DBCO **1** was functionalized with azido allyl sulfide **2** and the cell adhesive azido-RGDS peptide **3** and four-armed PEG<sub>20K</sub>-azide **4** on an azide-functionalized coverslip; B, Schematic of the Thiol-ene reaction between a Thiol radical-containing protein and the allyl sulfide moiety; C, Sequential tethering and release of multiple proteins with 3D control; Panels from the left to the right: Thiolated ovalbumin (AlexaFluor 555 conjugate, red) was uniformly tethered to the hydrogel; Selective release using PEG1K-thiol; "Coordinate axes" shape of thiolated transferrin (AlexaFluor 488 conjugate, green) was patterned within the volume of released ovalbumin; Two-photon photolithography enabled the patterning with 3D control. Scale bars 100  $\mu\text{m}$ . Reproduced from Reference [136] under the permission of American Chemical Society. D, NMT-Catalyzed Myristoylation of PhoCl fusions bearing the N-Terminal signaling sequence with 12-ADA in E, yields the site-specific incorporation of the azido functionality. E, Fluorescence from PhoCl (green) co-localized with that from mRuby (red). Light-treated gel regions appeared black, owing to patterned photorelease of the fluorescent protein and PhoCl's cleavage-associated loss of fluorescence. Images correspond to a single z slice from stacks acquired by fluorescence confocal microscopy. Scale bar = 200  $\mu\text{m}$ . Reproduced from Reference [137] under the permission of American Chemical Society

photopatterning and photorelease was developed using proteins site-specifically modified with a sortase-tag.<sup>[139]</sup> To enable photorelease, proteins were tagged with azide-functionalized ortho-nitrobenzyl ester moieties, which undergo rapid photocleavage at  $\lambda = 365 \text{ nm}$ ,<sup>[125]</sup> and tethered first uniformly in the SPAAC-PEG hydrogels. Photoligation was enabled using incorporation of a photocaged alkoxyamine, which permitted a localized immobilization of aldehyde-functionalized proteins. Using the combination of both approaches, protein photorelease could be performed along with photomediated ligation. The photopatterning process was successfully used to pattern and release growth factors permitting temporal control of cellular uptake and downstream response.<sup>[140]</sup>

#### 4 | CONCLUSION AND OUTLOOK

Protein-based materials can be produced in a variety of pattern from the nano to the macro scale. Due to their natural properties, including biocompatibility and biodegradability, proteins are a sustainable

alternative to synthetic polymers in their use as photoresists. In addition, proteins can be genetically or chemically modified to meet further requirements for material's research. Several disciplines such as food packaging, optics, electronics, drug delivery, tissue engineering, biomedical implantation and many others are covered. The use of adapted manufacturing methods and the optimization of processing parameters enables the production of outstanding materials for future applications.

Nonspecific adhesion and nonoriented covalent binding have been continuously used to establish new patterning approaches for protein immobilization. Main progress was achieved in the production of photocatalytically polymerized brushes leading to protein-repellant/adhesive patches enabling spatially defined protein adhesion on substrates. However, due to the uncontrollable orientation of the immobilized proteins, these approaches are less suitable for enzymes or ligand binding proteins, where inaccessibility of the active site can critically compromise the functionality of the patterned construct. Therefore, immobilization strategies on surface pattern with predefined configurations are significantly important for the production of biosensors and protein microarrays. Progress has been made by site-specific protein modifications, enzymatic introduction of

biorthogonal groups and/or photocaged reactive groups together with advanced photolithography strategies exposing corresponding coupling partners. These strategies allow for a spatially and temporally controlled construction of multi-pattern of highly oriented active proteins. The use of photocatalysts that are sensitive to noninvasive VIS and near-IR wavelengths is also considered more often to maintain the functionality of the proteins during the production process of the protein pattern. Promising approaches are the use of light-sensitive proteins that change their binding valences when absorbing visible light. Further improvements have been achieved using hydrogels immobilized on surfaces to create native-like protein environments. Here, the use of modern high-resolution photolithographic techniques and side-specific immobilization strategies allows the creation of highly controlled micro-environments to solve issues in cell biology and tissue engineering.

### ACKNOWLEDGEMENTS

This work was financially supported by the DFG grant SCHE 603/24-1 and Bayrisch-Tschechische Hochschulagentur grant JC-2019-21. Open Access funding enabled and organized by ProjektDEAL.

### CONFLICT OF INTEREST

The authors declare no competing interests.

### DATA AVAILABILITY STATEMENT

Data sharing not applicable to this article as no datasets were generated.

### ORCID

Martin Humenik  <https://orcid.org/0000-0002-2097-8941>

Thomas Scheibel  <https://orcid.org/0000-0002-0457-2423>

### REFERENCES

- [1] D. G. Bucknall, in *Nanolithography and patterning techniques in micro-electronics* (Ed: D. G. Bucknall), Woodhead Publishing, Cambridge, UK **2005**, p. 424.
- [2] A. Bernard, E. Delamarche, H. Schmid, B. Michel, H. R. Bosshard, H. Biebuyck, *Langmuir* **1998**, *14*, 2225.
- [3] J. Voskuhl, J. Brinkmann, P. Jonkheijm, *Curr. Opin. Chem. Biol.* **2014**, *18*, 1.
- [4] S. Alom Ruiz, C. S. Chen, *Soft Matter* **2007**, *3*, 168.
- [5] S. R. Coyer, A. J. García, E. Delamarche, *Angew. Chem., Int. Ed.* **2007**, *46*, 6837.
- [6] R. Kargl, T. Mohan, S. Köstler, S. Spirk, A. Doliška, K. Stana-Kleinschek, V. Ribitsch, *Adv. Funct. Mater.* **2013**, *23*, 308.
- [7] E. Gdor, S. Shemesh, S. Magdassi, D. Mandler, *ACS Appl. Mater. Interfaces* **2015**, *7*, 17985.
- [8] S. Marchesan, C. D. Easton, K. E. Styan, P. Leech, T. R. Gengenbach, J. S. Forsythe, P. G. Hartley, *Colloids Surf., B* **2013**, *108*, 313.
- [9] R. E. Alvarado, H. T. Nguyen, B. Pepin-Donat, C. Lombard, Y. Roupioz, L. Leroy, *Langmuir* **2017**, *33*, 10511.
- [10] Y. L. Jeyachandran, N. Meyerbröker, A. Terfort, M. Zharnikov, *J. Phys. Chem. C* **2015**, *119*, 494.
- [11] A. M. Alswieleh, N. Cheng, I. Canton, B. Ustbas, X. Xue, V. Ladmiral, S. Xia, R. E. Ducker, O. El Zubir, M. L. Cartron, C. N. Hunter, G. J. Leggett, S. P. Armes, *J. Am. Chem. Soc.* **2014**, *136*, 9404.
- [12] N. Ballav, H. Thomas, T. Winkler, A. Terfort, M. Zharnikov, *Angew. Chem., Int. Ed.* **2009**, *48*, 5833.
- [13] S. Kim, B. Marelli, M. A. Brenckle, A. N. Mitropoulos, E.-S. Gil, K. Tsioris, H. Tao, D. L. Kaplan, F. G. Omenetto, *Nat. Nanotechnol.* **2014**, *9*, 306.
- [14] K.-B. Lee, S.-J. Park, C. A. Mirkin, J. C. Smith, M. Mrksich, *Science* **2002**, *295*, 1702.
- [15] J. Chai, L. S. Wong, L. Giam, C. A. Mirkin, *Proc. Natl. Acad. Sci. U. S. A.* **2011**, *108*, 19521.
- [16] A. B. Braunschweig, F. Huo, C. A. Mirkin, *Nat. Chem.* **2009**, *1*, 353.
- [17] G. Liu, S. H. Petrosko, Z. Zheng, C. A. Mirkin, *Chem. Rev.* **2020**, *120*, 6009.
- [18] C. Vasilev, M. P. Johnson, E. Gonzales, L. Wang, A. V. Ruban, G. Montano, A. J. Cadby, C. N. Hunter, *Langmuir* **2014**, *30*, 8481.
- [19] D. Falconnet, D. Pasqui, S. Park, R. Eckert, H. Schiff, J. Gobrecht, R. Barbucci, M. Textor, *Nano Lett.* **2004**, *4*, 1909.
- [20] R. V. Martínez, J. Martínez, M. Chiesa, R. Garcia, E. Coronado, E. Pinilla-Cienfuegos, S. Tatay, *Adv. Mater.* **2010**, *22*, 588.
- [21] J. Shi, J. Chen, P. S. Cremer, *J. Am. Chem. Soc.* **2008**, *130*, 2718.
- [22] M. Montague, R. E. Ducker, K. S. L. Chong, R. J. Manning, F. J. M. Rutten, M. C. Davies, G. J. Leggett, *Langmuir* **2007**, *23*, 7328.
- [23] E. Ul-Haq, S. Patole, M. Moxey, E. Amstad, C. Vasilev, C. N. Hunter, G. J. Leggett, N. D. Spencer, N. H. Williams, *ACS Nano* **2013**, *7*, 7610.
- [24] D. Weinrich, P. Jonkheijm, C. M. Niemeyer, H. Waldmann, *Angew. Chem., Int. Ed.* **2009**, *48*, 7744.
- [25] M. Ventre, F. Causa, P. A. Netti, *J. Royal Soc. Interface* **2012**, *9*, 2017.
- [26] A. Khademhosseini, R. Langer, J. Borenstein, J. P. Vacanti, *Proc. Natl. Acad. Sci. U. S. A.* **2006**, *103*, 2480.
- [27] J. Yeo, G. Jung, A. Tarakanova, F. J. Martin-Martinez, Z. Qin, Y. Cheng, Y.-W. Zhang, M. J. Buehler, *Extreme Mech. Lett.* **2018**, *20*, 112.
- [28] F. Costa, R. Silva, A. R. Boccaccini, Fibrous protein-based biomaterials (silk, keratin, elastin, and resilin proteins) for tissue regeneration and repair in Peptides and proteins as biomaterials for tissue regeneration and repair, **2018**; p 175.
- [29] Z. Zhou, S. Zhang, Y. Cao, B. Marelli, X. Xia, T. H. Tao, *Adv. Mater.* **2018**, *30*, e1706983.
- [30] B. Zhu, H. Wang, W. R. Leow, Y. Cai, X. J. Loh, M. Y. Han, X. Chen, *Adv. Mater.* **2016**, *28*, 4250.
- [31] W. Huang, S. Ling, C. Li, F. G. Omenetto, D. L. Kaplan, *Chem. Soc. Rev.* **2018**, *47*, 6486.
- [32] L. D. Koh, J. Yeo, Y. Y. Lee, Q. Ong, M. Han, B. C. Tee, *Mater. Sci. Eng., C* **2018**, *86*, 151.
- [33] G. Tullii, S. Donini, C. Bossio, F. Lodola, M. Pasini, E. Parisini, F. Galeotti, M. R. Antognazza, *ACS Appl. Mater. Interfaces* **2020**, *12*, 5437.
- [34] B. Ganesh Kumar, R. Melikov, M. Mohammadi Aria, A. Ural Yalcin, E. Begar, S. Sadeghi, K. Guven, S. Nizamoglu, *ACS Biomater. Sci. Eng.* **2018**, *4*, 1463.
- [35] Y. Sun, Q. Jallerat, J. M. Szymanski, A. W. Feinberg, *Nat. Methods* **2015**, *12*, 134.
- [36] J. Park, S.-G. Lee, B. Marelli, M. Lee, T. Kim, H.-K. Oh, H. Jeon, F. G. Omenetto, S. Kim, *RSC Adv.* **2016**, *6*, 39330.
- [37] Y. Wang, B. J. Kim, B. Peng, W. Li, Y. Wang, M. Li, F. G. Omenetto, *Proc. Natl. Acad. Sci. U. S. A.* **2019**, *116*, 21361.
- [38] Y. L. Sun, Q. Li, S. M. Sun, J. C. Huang, B. Y. Zheng, Q. D. Chen, Z. Z. Shao, H. B. Sun, *Nat. Commun.* **2015**, *6*, 8612.
- [39] D. Sanchez-Dealcazar, D. Romera, J. Castro-Smirnov, A. Sousaraei, S. Casado, A. Espasa, M. C. Morant-Miñana, J. J. Hernandez, I. Rodriguez, R. D. Costa, J. Cabanillas-Gonzalez, R. V. Martinez, A. L. Cortajarena, *Nanoscale Adv.* **2019**, *1*, 3980.
- [40] M. B. Applegate, B. P. Partlow, J. Coburn, B. Marelli, C. Pirie, R. Pineda, D. L. Kaplan, F. G. Omenetto, *Adv. Mater.* **2016**, *28*, 2417.

- [41] A. Brif, P. Laity, F. Claeysens, C. Holland, *ACS Biomater. Sci. Eng.* **2019**, *6*, 705.
- [42] A. Bettadapur, G. C. Suh, N. A. Geisse, E. R. Wang, C. Hua, H. A. Huber, A. A. Viscio, J. Y. Kim, J. B. Strickland, M. L. McCain, *Sci. Rep.* **2016**, *6*, 28855.
- [43] J. Jiang, S. Zhang, Z. Qian, N. Qin, W. Song, L. Sun, Z. Zhou, Z. Shi, L. Chen, X. Li, Y. Mao, D. L. Kaplan, S. N. Gilbert Corder, X. Chen, M. Liu, F. G. Omenetto, X. Xia, T. H. Tao, *Adv. Mater.* **2018**, *30*, 1705919.
- [44] Y. Li, K. Li, X. Wang, B. An, M. Cui, J. Pu, S. Wei, S. Xue, H. Ye, Y. Zhao, M. Liu, Z. Wang, C. Zhong, *Nano Lett.* **2019**, *19*, 8399.
- [45] N. Van Gerven, R. D. Klein, S. J. Hultgren, H. Remaut, *Trends Microbiol.* **2015**, *23*, 693.
- [46] A. Pena-Francesch, S. Florez, H. Jung, A. Sebastian, I. Albert, W. Curtis, M. C. Demirel, *Adv. Funct. Mater.* **2014**, *24*, 7401.
- [47] A. Pena-Francesch, N. E. Domeradzka, H. Jung, B. Barbu, M. Vural, Y. Kikuchi, B. D. Allen, M. C. Demirel, *APL Mater.* **2018**, *6*, 010701.
- [48] H. Yilmaz, A. Pena-Francesch, R. Shreiner, H. Jung, Z. Belay, M. C. Demirel, Ş. K. Özdemir, L. Yang, *ACS Photonics* **2017**, *4*, 2179.
- [49] A. Paul, M. Stührenberg, S. Chen, D. Rhee, W. K. Lee, T. W. Odom, S. C. Heilshorn, A. Enejder, *Soft Matter* **2017**, *13*, 5665.
- [50] M. Cavallini, C. Albonetti, F. Biscarini, *Adv. Mater.* **2009**, *21*, 1043.
- [51] F. Bauer, S. Wohlrab, T. Scheibel, *Biomater. Sci.* **2013**, *1*, 1244.
- [52] S. Kumari, G. Lang, E. Desimone, C. Spengler, V. T. Trossmann, S. Lücker, M. Hudel, K. Jacobs, N. Krämer, T. Scheibel, *Mater. Today* **2020**.
- [53] S. Kumari, G. Lang, E. Desimone, C. Spengler, V. T. Trossmann, S. Lücker, M. Hudel, K. Jacobs, N. Krämer, T. Scheibel, *Data Brief* **2020**, *32*, 106305.
- [54] N. E. Kurland, T. Dey, S. C. Kundu, V. K. Yadavalli, *Adv. Mater.* **2013**, *25*, 6207.
- [55] N. E. Kurland, T. Dey, C. Wang, S. C. Kundu, V. K. Yadavalli, *Adv. Mater.* **2014**, *26*, 4431.
- [56] A. R. Parker, H. E. Townley, *Nat. Nanotechnol.* **2007**, *2*, 347.
- [57] R. K. Pal, N. E. Kurland, C. Wang, S. C. Kundu, V. K. Yadavalli, *ACS Appl. Mater. Interfaces* **2015**, *7*, 8809.
- [58] A. Bucciarelli, R. K. Pal, D. Maniglio, A. Quaranta, V. Mulloni, A. Motta, V. K. Yadavalli, *Macromol. Mater. Eng.* **2017**, *302*, 1700110.
- [59] W. Liu, Z. Zhou, S. Zhang, Z. Shi, J. Tabarini, W. Lee, Y. Zhang, S. N. Gilbert Corder, X. Li, F. Dong, L. Cheng, M. Liu, D. L. Kaplan, F. G. Omenetto, G. Zhang, Y. Mao, T. H. Tao, *Adv. Sci. (Weinheim, Ger.)* **2017**, *4*, 1700191.
- [60] R. K. Pal, A. A. Farhaly, M. M. Collinson, S. C. Kundu, V. K. Yadavalli, *Adv. Mater.* **2016**, *28*, 1406.
- [61] M. Xu, S. Pradhan, F. Agostinacchio, R. K. Pal, G. Greco, B. Mazzolai, N. M. Pugno, A. Motta, V. K. Yadavalli, *Adv. Mater. Interfaces* **2019**, *6*, 1801822.
- [62] S. Zhu, W. Zeng, Z. Meng, W. Luo, L. Ma, Y. Li, C. Lin, Q. Huang, Y. Lin, X. Y. Liu, *Adv. Mater.* **2019**, *31*, e1900870.
- [63] S. M. Kim, M. Ueki, X. Ren, J. Akimoto, Y. Sakai, Y. Ito, *Int. J. Nanomed.* **2019**, *14*, 7683.
- [64] S. Morlat, J.-L. Gardette, *Polymer* **2003**, *44*, 7891.
- [65] P.-O. Strale, A. Azioune, G. Bugnicourt, Y. Lecomte, M. Chahid, V. Studer, *Adv. Mater.* **2016**, *28*, 2024.
- [66] C. Xie, W. Sun, H. Lu, A. Kretzschmann, J. Liu, M. Wagner, H.-J. Butt, X. Deng, S. Wu, *Nat. Commun.* **2018**, *9*, 3842.
- [67] O. El Zubir, S. Xia, R. E. Ducker, L. Wang, N. Mullin, M. L. Cartron, A. J. Cadby, J. K. Hobbs, C. N. Hunter, G. J. Leggett, *Langmuir* **2017**, *33*, 8829.
- [68] M. Moxey, A. Johnson, O. El-Zubir, M. Cartron, S. S. Dinachali, C. N. Hunter, M. S. M. Saifullah, K. S. L. Chong, G. J. Leggett, *ACS Nano* **2015**, *9*, 6262.
- [69] T. L. Rapp, C. A. Deforest, *Adv. Healthcare Mater.* **2020**, *9*, 1901553.
- [70] Z. Chen, S. He, H.-J. Butt, S. Wu, *Adv. Mater.* **2015**, *27*, 2203.
- [71] X. Liu, M. Kumar, A. Calo, E. Albisetti, X. Zheng, K. B. Manning, E. Elacqua, M. Weck, R. V. Ulijn, E. Riedo, *Faraday Discuss.* **2019**, *219*, 33.
- [72] P. Yang, *Macromol. Biosci.* **2012**, *12*, 1053.
- [73] Z. Wu, P. Yang, *Adv. Mater. Interfaces* **2015**, *2*, 1400401.
- [74] N. Gupta, B. F. Lin, L. M. Campos, M. D. Dimitriou, S. T. Hikita, N. D. Treat, M. V. Tirrell, D. O. Clegg, E. J. Kramer, C. J. Hawker, *Nat. Chem.* **2010**, *2*, 138.
- [75] W. Feng, L. Li, E. Ueda, J. Li, S. Heißler, A. Welle, O. Trapp, P. A. Levkin, *Adv. Mater. Interfaces* **2014**, *1*, 1400269.
- [76] R. Zandi Shafagh, A. Vastesson, W. Guo, W. Van Der Wijngaart, T. Haraldsson, *ACS Nano* **2018**, *12*, 9940.
- [77] H. Ma, A. S. Caldwell, M. A. Azagarsamy, A. Gonzalez Rodriguez, K. S. Anseth, *Biomaterials* **2020**, *255*, 120205.
- [78] K. Y. Tan, M. Ramstedt, B. Colak, W. T. S. Huck, J. E. Gautrot, *Polym. Chem.* **2016**, *7*, 979.
- [79] C.-F. Huang, *Polym. J. (Tokyo, Jpn.)* **2016**, *48*, 341.
- [80] X. Meng, J. Hu, Z. Chao, Y. Liu, H. Ju, Q. Cheng, *ACS Appl. Mater. Interfaces* **2018**, *10*, 1324.
- [81] S. G. Ricoult, A. Sanati Nezhad, M. Knapp-Mohammady, T. E. Kennedy, D. Juncker, *Langmuir* **2014**, *30*, 12002.
- [82] Y. X. And, G. M. Whitesides, *Annu. Rev. Mater. Sci.* **1998**, *28*, 153.
- [83] G. M. Whitesides, E. Ostuni, S. Takayama, X. Jiang, D. E. Ingber, *Annu. Rev. Biomed. Eng.* **2001**, *3*, 335.
- [84] C. Dirscherl, S. Springer, *Eng. Life Sci.* **2018**, *18*, 124.
- [85] H. Lee, S. M. Dellatore, W. M. Miller, P. B. Messersmith, *Science* **2007**, *318*, 426.
- [86] H.-W. Chien, W.-H. Kuo, M.-J. Wang, S.-W. Tsai, W.-B. Tsai, *Langmuir* **2012**, *28*, 5775.
- [87] Q. Wei, T. Becherer, S. Angioletti-Uberti, J. Dzubiella, C. Wischke, A. T. Neffe, A. Lendlein, M. Ballauff, R. Haag, *Angew. Chem., Int. Ed.* **2014**, *53*, 8004.
- [88] B. Vonhören, M. Langer, D. Abt, C. Barner-Kowollik, B. J. Ravoo, *Langmuir* **2015**, *31*, 13625.
- [89] H. Zhao, J. Sha, T. Wu, T. Chen, X. Chen, H. Ji, Y. Wang, H. Zhu, L. Xie, Y. Ma, *Appl. Surf. Sci.* **2020**, *529*, 147056.
- [90] U. Bog, A. De Los Santos, S. L. Pereira, S. Mueller, V. Havenridge, M. Parrillo, A. E. Bruns, C. Holmes, H. Rodriguez-Emmenegger, M. H. Fuchs, *ACS Appl. Mater. Interfaces* **2017**, *9*, 12109.
- [91] E. Bat, J. Lee, U. Y. Lau, H. D. Maynard, *Nat. Commun.* **2015**, *6*, 6654.
- [92] U. Y. Lau, S. S. Saxer, J. Lee, E. Bat, H. D. Maynard, *ACS Nano* **2016**, *10*, 723.
- [93] Y. Liu, J. Yu, *Microchim. Acta* **2016**, *183*, 1.
- [94] P. Jonkheijm, D. Weinrich, H. Schröder, C. M. Niemeyer, H. Waldmann, *Angew. Chem., Int. Ed.* **2008**, *47*, 9618.
- [95] A. Sassolas, L. J. Blum, B. D. Leca-Bouvier, *Biotechnol. Adv.* **2012**, *30*, 489.
- [96] P.-C. Lin, D. Weinrich, H. Waldmann, *Macromol. Chem. Phys.* **2010**, *211*, 136.
- [97] E. M. Sletten, C. R. Bertozzi, *Angew. Chem., Int. Ed.* **2009**, *48*, 6974.
- [98] E. A. Hoyt, P. M. S. D. Cal, B. L. Oliveira, G. J. L. Bernardes, *Nat. Rev. Chem.* **2019**, *3*, 147.
- [99] J. A. Shadish, C. A. Deforest, *Matter* **2020**, *2*, 50.
- [100] J. A. Bornhorst, J. J. Falke, *Purification of proteins using polyhistidine affinity tags in Methods enzymol.*, Vol. 326, Academic Press, Cambridge, MA, USA **2000**, p. 245. Ch. 16.
- [101] L. Nieba, S. E. Nieba-Axmann, A. Persson, M. Hämäläinen, F. Edebratt, A. Hansson, J. Lidholm, K. Magnusson, Å. F. Karlsson, A. Plückthun, *Anal. Biochem.* **1997**, *252*, 217.
- [102] D. Kröger, M. Liley, W. Schiweck, A. Skerra, H. Vogel, *Biosens. Bioelectron.* **1999**, *14*, 155.
- [103] S. Xia, M. Cartron, J. Morby, D. A. Bryant, C. N. Hunter, G. J. Leggett, *Langmuir* **2016**, *32*, 1818.

- [104] L. Liu, J. A. Shadish, C. K. Arakawa, K. Shi, J. Davis, C. A. Deforest, *Adv. Biosyst.* **2018**, *2*, 1800240.
- [105] S. Lyu, J. Fang, T. Duan, L. Fu, J. Liu, H. Li, *Chem. Commun. (Camb.)* **2017**, *53*, 13375.
- [106] M. Hörner, K. Raute, B. Hummel, J. Madl, G. Creusen, O. S. Thomas, E. H. Christen, N. Hotz, R. J. Gübeli, R. Engesser, B. Rebmann, J. Lauer, B. Rolauffs, J. Timmer, W. W. A. Schamel, J. Pruszk, W. Römer, M. D. Zurbriggen, C. Friedrich, A. Walther, S. Minguet, R. Sawarkar, W. Weber, *Adv. Mater.* **2019**, *31*, 1806727.
- [107] D. Xu, S. M. Bartelt, S. Rasoulinejad, F. Chen, S. V. Wegner, *Mater. Horiz.* **2019**, *6*, 1222.
- [108] D. Wasserberg, J. Cabanas-Danés, J. Prangma, S. O'mahony, P.-A. Cazade, E. Tromp, C. Blum, D. Thompson, J. Huskens, V. Subramaniam, P. Jonkheijm, *ACS Nano* **2017**, *11*, 9068.
- [109] S. C. Reddington, M. Howarth, *Curr. Opin. Chem. Biol.* **2015**, *29*, 94.
- [110] G. Veggiani, T. Nakamura, M. D. Brenner, R. V. Gayet, J. Yan, C. V. Robinson, M. Howarth, *Proc. Natl. Acad. Sci. U. S. A.* **2016**, *113*, 1202.
- [111] D. M. Williams, G. Kaufman, H. Izadi, A. E. Gahm, S. M. Prophet, K. T. Vanderlick, C. O. Osuji, L. Regan, *ACS Appl. Nano Mater.* **2018**, *1*, 2483.
- [112] K. Zhou, J. Dong, Y. Zhou, J. Dong, M. Wang, Q. Wang, *Small* **2019**, *15*, 1804044.
- [113] R. Meyer, S. Giselbrecht, B. E. Rapp, M. Hirtz, C. M. Niemeyer, *Curr. Opin. Chem. Biol.* **2014**, *18*, 8.
- [114] C. M. Niemeyer, *Angew. Chem., Int. Ed.* **2010**, *49*, 1200.
- [115] A. Kerbs, P. Mueller, M. Kaupp, I. Ahmed, A. S. Quick, D. Abt, M. Wegener, C. M. Niemeyer, C. Barner-Kowollik, L. Fruk, *Chem. - Eur. J.* **2017**, *23*, 4990.
- [116] L. Feng, J. Romulus, M. Li, R. Sha, J. Royer, K.-T. Wu, Q. Xu, N. C. Seeman, M. Weck, P. Chaikin, *Nat. Mater.* **2013**, *12*, 747.
- [117] F. Huang, H. Xu, W. Tan, H. Liang, *ACS Nano* **2014**, *8*, 6849.
- [118] Y. Song, T. Takahashi, S. Kim, Y. C. Heaney, J. Warner, S. Chen, M. J. Heller, *ACS Appl. Mater. Interfaces* **2017**, *9*, 22.
- [119] M. Humenik, T. Scheibel, *ACS Nano* **2014**, *8*, 1342.
- [120] M. Humenik, T. Preiß, S. Gödrich, G. Papastavrou, T. Scheibel, *Mater. Today Bio* **2020**, *6*, 100045.
- [121] A. Molina, T. Scheibel, M. Humenik, *Biomacromolecules* **2019**, *20*, 347.
- [122] Y. S. Zhang, A. Khademhosseini, *Science* **2017**, *356*, eaaf3627.
- [123] I. Y. Jung, J. S. Kim, B. R. Choi, K. Lee, H. Lee, *Adv. Healthcare Mater.* **2017**, *6*, 1601475.
- [124] R. V. Ulijn, N. Bibi, V. Jayawarna, P. D. Thornton, S. J. Todd, R. J. Mart, A. M. Smith, J. E. Gough, *Mater. Today* **2007**, *10*, 40.
- [125] C. A. Deforest, D. A. Tirrell, *Nat. Mater.* **2015**, *14*, 523.
- [126] A. Shastri, L. M. Mcgregor, Y. Liu, V. Harris, H. Nan, M. Mujica, Y. Vasquez, A. Bhattacharya, Y. Ma, M. Aizenberg, O. Kuksenok, A. C. Balazs, J. Aizenberg, X. He, *Nat. Chem.* **2015**, *7*, 447.
- [127] C. D. Blanchette, J. M. Knipe, J. K. Stolaroff, J. R. Deotte, J. S. Oakdale, A. Maiti, J. M. Lenhardt, S. Sirajuddin, A. C. Rosenzweig, S. E. Baker, *Nat. Commun.* **2016**, *7*, 11900.
- [128] A. M. Horgan, J. D. Moore, J. E. Noble, G. J. Worsley, *Trends Biotechnol.* **2010**, *28*, 485.
- [129] G. C. Le Goff, R. L. Srinivas, W. A. Hill, P. S. Doyle, *Eur. Polym. J.* **2015**, *72*, 386.
- [130] A. K. Gaharwar, I. Singh, A. Khademhosseini, *Nat. Rev. Mater.* **2020**, *5*, 686.
- [131] C. N. Lafratta, J. T. Fourkas, T. Baldacchini, R. A. Farrer, *Angew. Chem., Int. Ed.* **2007**, *46*, 6238.
- [132] M. A. Skylar-Scott, M.-C. Liu, Y. Wu, A. Dixit, M. F. Yanik, *Adv. Healthcare Mater.* **2016**, *5*, 1233.
- [133] J. H. Wosnick, M. S. Shoichet, *Chem. Mater.* **2008**, *20*, 55.
- [134] M. B. Dickerson, P. B. Dennis, V. P. Tondiglia, L. J. Nadeau, K. M. Singh, L. F. Drummy, B. P. Partlow, D. P. Brown, F. G. Omenetto, D. L. Kaplan, R. R. Naik, *ACS Biomater. Sci. Eng.* **2017**, *3*, 2064.
- [135] Z. Ming, X. Ruan, C. Bao, Q. Lin, Y. Yang, L. Zhu, *Adv. Funct. Mater.* **2017**, *27*, 1606258.
- [136] J. C. Grim, T. E. Brown, B. A. Aguado, D. A. Chapnick, A. L. Viert, X. Liu, K. S. Anseth, *ACS Cent. Sci.* **2018**, *4*, 909.
- [137] J. A. Shadish, A. C. Strange, C. A. Deforest, *J. Am. Chem. Soc.* **2019**, *141*, 15619.
- [138] Z. Ming, J. Fan, C. Bao, Y. Xue, Q. Lin, L. Zhu, *Adv. Funct. Mater.* **2018**, *28*, 1706918.
- [139] H. Mao, S. A. Hart, A. Schink, B. A. Pollok, *J. Am. Chem. Soc.* **2004**, *126*, 2670.
- [140] J. A. Shadish, G. M. Benuska, C. A. Deforest, *Nat. Mater.* **2019**, *18*, 1005.

## AUTHOR BIOGRAPHIES



**MARTIN HUMENIK** received his Diploma (2000) and PhD (2005) in organic chemistry at the University of P. J. Safarik in Kosice, Slovakia. He was a post-doc in Prof. Mathias Sprinzl's laboratories in the Department of Biochemistry at the Universität Bayreuth, Germany (2005-2009). In 2009 he joined the laboratories of Prof. Thomas Scheibel as a senior researcher in the Department of Biomaterials, Universität Bayreuth. His research focuses on protein- and DNA-based self-assembling materials.



**ANIKA WINKLER** received her Bachelor's degree in biochemistry and Master's degree in biochemistry and molecular biology from the Universität Bayreuth, Germany. She is currently a PhD candidate at the Universität Bayreuth under the supervision of Prof. Thomas Scheibel. Her current research is centred on the development and production of adhesive proteins for medical applications.



**THOMAS SCHEIBEL** has been a full professor in the Department of Biomaterials at the Universität Bayreuth, Germany since 2007. He received both his Diploma of Biochemistry (1994) and a Dr rer. nat. (1998) from the Universität Regensburg, Germany. After postdoctoral work at the University of Chicago, U.S.A. (1998-2001), he received habilitation from the Technische Universität München, Germany (2007). His research focuses on biotechnological production and processing of structural proteins, as well as biomedical and technical applications of protein-based materials.

**How to cite this article:** Humenik M, Winkler A, Scheibel T. Patterning of protein-based materials. *Biopolymers*. 2020; e23412. <https://doi.org/10.1002/bip.23412>